JACS
JOURNAL OF THE AMERICAN CHEMICAL SOCIETY

Communication

pubs.acs.org/JACS

The Organic Secondary Building Unit: Strong Intermolecular π Interactions Define Topology in MIT-25, a Mesoporous MOF with Proton-Replete Channels

Sarah S. Park,[†] Christopher H. Hendon,[†] Alistair J. Fielding,[‡] Aron Walsh,[§,∥] Michael O'Keeffe,[⊥] and Mircea Dincă*[,†]

[†]Department of Chemistry, Massachusetts Institute of Technology, 77 Massachusetts Avenue, Cambridge, Massachusetts 02139, United States

[‡]School of Chemistry and the Photon Science Institute, The University of Manchester, Manchester M13 9PL, United Kingdom

[§]Department of Materials, Imperial College London, London SW7 2AZ, United Kingdom

[∥]Department of Materials Science and Engineering, Yonsei University, Seoul 03722, South Korea

[⊥]School of Molecular Sciences, Arizona State University, Tempe, Arizona 85287, United States

Supporting Information

ABSTRACT: The structure-directing role of the inorganic secondary building unit (SBU) is key for determining the topology of metal−organic frameworks (MOFs). Here we show that organic building units relying on strong π interactions that are energetically competitive with the formation of common inorganic SBUs can also play a role in defining the topology. We demonstrate the importance of the *organic* SBU in the formation of $Mg_2H_6(H_3O)(TTFTB)_3$ (**MIT-25**), a mesoporous MOF with the new **ssp** topology. A delocalized electronic hole is critical in the stabilization of the TTF triad organic SBUs and exemplifies a design principle for future MOF synthesis.

The topology of a metal−organic framework (MOF) is dictated by the geometries of both the inorganic secondary building units (SBUs) and the ligands. Predicting the topology by combining SBUs and ligands with predefined geometries is a feature of reticular chemistry.[1] It has allowed the synthesis of thousands of new materials with increasingly complex topologies even though the experimental conditions that lead to the self-assembly of a given inorganic SBU are largely empirical. The premise of reticular chemistry is that most common SBUs are thermodynamic sinks whose formation and structure are rarely disturbed by non-covalent interactions. However, because reticular chemistry relies on strong directional bonding between ligands and metals/metal clusters, its predictions break down when non-covalent interactions compete energetically with coordination bonds. This results in surprising and often new topologies.

We have set out to learn whether we can predict when thermodynamic products are likely to deviate from those predicted by reticular chemistry and what are the causes that lead to these exceptions. We have further ventured to test whether the non-covalent interactions that prevent the formation of empirically expected SBUs may be used to direct topology themselves. This would provide access to new materials and contribute to a deeper understanding of the physical principles governing MOF synthesis.

Here we report the synthesis and characterization of a new three-dimensionally connected MOF, $Mg_2H_6(H_3O)(TTFTB)_3$ (TTFTB = tetrathiafulvalene-tetrabenzoate), denoted as **MIT-25**, whose topology is defined by strong intermolecular π and hydrogen-bonding interactions. **MIT-25** exhibits permanent 26.4 Å × 30.5 Å mesopores running parallel to smaller pores occluded by hydronium ions. Controlling the topology by employing π-stacked organic supramolecular building blocks[2] (i.e., organic SBUs) serves as a powerful paradigm for the design of novel hybrid frameworks.

In some cases, π interactions provide a stabilization energy of at least −13.0 kcal/mol,[3] which is far greater than that of hydrogen bonding in water (1−6 kcal/mol depending on the conditions)[4] and comparable to some metal−ligand bonds[5] frequently found in MOFs. It is therefore conceivable that using ligands with a high propensity for strong π interactions will be competitive with the self-assembly of canonical inorganic SBUs, leading instead to the formation of unusual topologies centered around the organic SBUs. Hints that strong π interactions can influence the topology of MOFs came from previous work with H_4TTFTB, which forms unusual helical stacks of TTF within frameworks made with transition metals.[6] We reasoned that reaction of this ligand with metals exhibiting even more ionic (i.e., weaker) metal−carboxylate bonds, such as Mg^{2+},[5] could promote the isolation of topologies where organic SBUs play prominent roles.

Reaction of H_4TTFTB with $Mg(NO_3)_2{\cdot}6H_2O$ in a mixture of *N*,*N*-dimethylformamide (DMF), water, and ethanol yielded red needles of $[Mg_2H_6(H_3O)(TTFTB)_3]{\cdot}1.5(DMF){\cdot}(H_2O)$, which crystallizes in space group $R\bar{3}$ (Figure 1a). Three TTFTB ligands form a tightly packed organic SBU with TTF···TTF distances of 3.73 Å. These triad organic SBUs do not form infinitely continuous intermolecular π stacks but rather exhibit close intertriad S···S contacts of 3.56 Å (Figure 1b and e). The 12

Received: December 22, 2016
Published: February 27, 2017

DOI: 10.1021/jacs.6b13176
J. Am. Chem. Soc. 2017, 139, 3619−3622

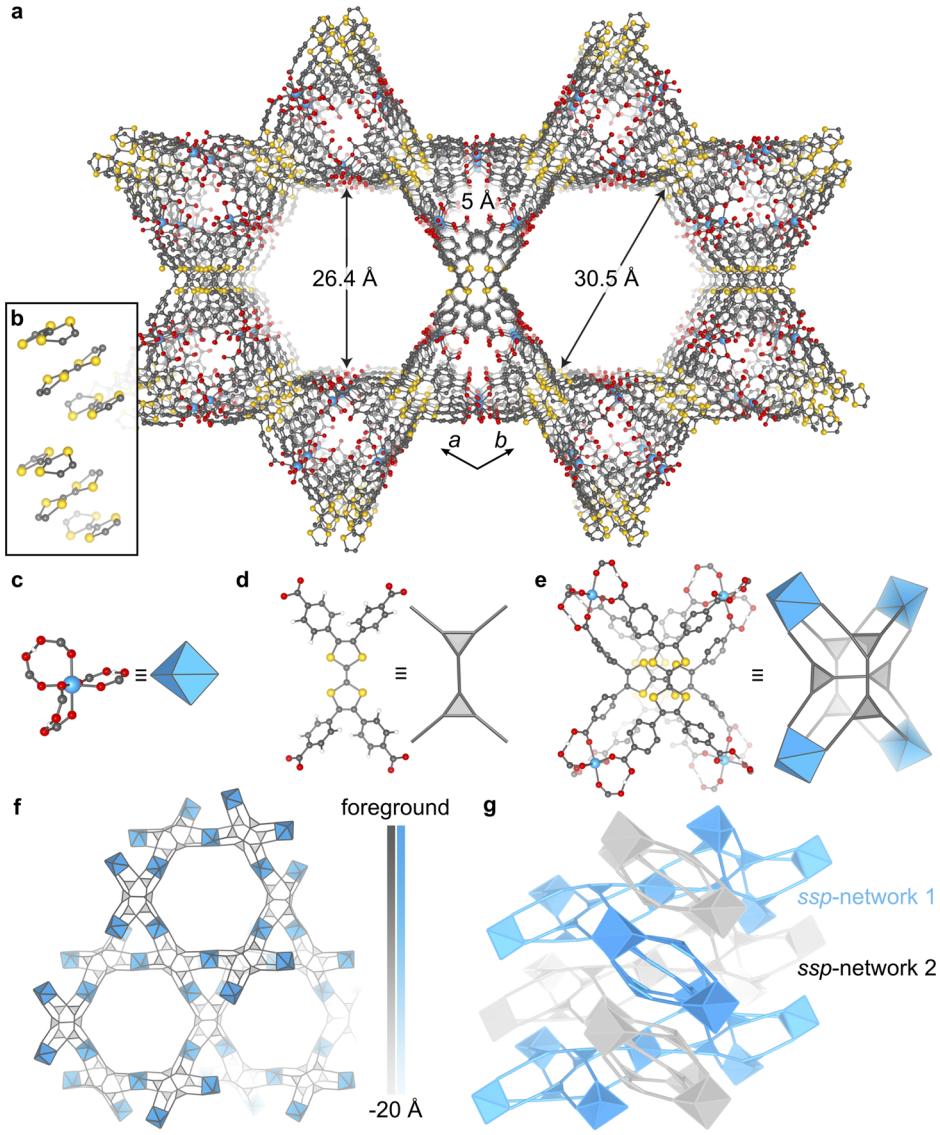

Figure 1. (a) A portion of the X-ray crystal structure of **MIT-25** featuring distinct mesopores. (b) The walls are constructed from TTF trimeric stacks aligned along the *c* axis. (c) The structure exhibits a mononuclear octahedral Mg^{2+} inorganic SBU supported by three additional protons that bridge pairs of carboxylate groups. (d) Ligand and metal nodes are represented by gray and blue shapes, respectively. (e) Four neighboring Mg^{2+} sites are linked by a TTFTB triad. (f) A representation of a single **ssp** net within **MIT-25**, exhibiting a "three-tier" hexagonal pore structure. (g) The small pore is helical, and the **ssp** net allows interpenetration of two densely woven frameworks, forming the terminal TTF stacks in the *c* direction.

carboxylates in each triad are connected to four Mg^{2+} ions, and each octahedral Mg^{2+} ion is connected facially to two independent triads. Although individual Mg^{2+} ions are separated by at least 10.23 Å, thereby forming monometallic inorganic SBUs, the coordination environment around each Mg^{2+} ion is further supported by three μ_2-protons that are shared between neighboring carboxylates bound to the same Mg^{2+} ion (Figure 1c).

The crystallographic positions of these shared protons could not be determined from X-ray diffraction analysis alone. Their position bridging between two oxygen atoms was assigned from density functional theory (DFT) calculations (Figure 1c). To explore this unusual SBU computationally, we constructed a cluster model, $[Mg(OAc)_6H_3]^-$ (Figure S1), which upon geometric relaxation converged to a tris-μ_2-H^+ conformation analogous to that observed in **MIT-25**. Importantly, omission of the μ_2 protons in this acetate-based model system resulted in the destruction of the octahedral coordination environment around Mg^{2+}, inferring that the protons serve both charge-balancing and structural roles.

Considering each TTFTB ligand as two three-connected nodes (Figure 1d) and each $MgH_3(O_2C-)_6$ unit as a six-connected node (Figure 1c), **MIT-25** self-assembles into the new **ssp** topology, a 3,3,6-connected net (Figure 1f). The **ssp** topology is most closely related to the **nbo** net (a comparison is presented in Figure S2). In **MIT-25**, two **ssp** nets are interpenetrated (Figure 1g) and define two channels parallel to the *c* axis with geometric pore apertures of 26.4 Å × 30.5 Å and 5.0 Å × 5.6 Å (Figures 1a and S3).

MIT-25 is permanently mesoporous. Thermogravimetric analysis (TGA) of as-synthesized material upon washing with DMF and ethanol followed by soaking in tetrahydrofuran (THF) revealed a plateau between approximately 100 and 200 °C (Figure S4). Heating a sample of **MIT-25** under vacuum at 200 °C followed by measurement of the N_2 adsorption isotherm at 77 K revealed a type-IV isotherm with a maximal N_2 uptake of

DOI: 10.1021/jacs.6b13176
J. Am. Chem. Soc. 2017, 139, 3619−3622

~330 cm^3/g. Barrett–Joyner–Halenda (BJH) pore size analysis[7] using the Kruk–Jaroniec–Sayari correction[8] for hexagonal pores and Brunauer–Emmett–Teller (BET)[9] fits to this isotherm revealed a pore size of 27.2 Å, in line with crystallographic analysis, and an apparent surface area of 830 m^2/g (Figures S5 and S6). The molar surface area, 1756 $m^2/mmol$, is also in line with those of other mesoporous MOFs with similar pore sizes.[10]

Formulating the inorganic SBUs as $[MgH_3(O_2C-)_6]^-$ and considering that there are two inorganic SBUs and one organic SBU (i.e., the three-ligand triad) in each formula unit, **MIT-25** would carry a doubly negative charge: $[Mg_2H_6(TTFTB)_3]^{2-}$. We employed electron paramagnetic resonance (EPR) spectroscopy to elucidate the nature of the charge-compensating species. Continuous-wave EPR spectra show that **MIT-25** is paramagnetic, exhibiting "powder" rhombic resonance patterns with principal g values of 2.014–2.010, 2.0061, and 2.002 at the turning points (Figure S8), consistent with sulfur-based radicals.[11] This assignment was confirmed by collecting spectra at two different frequencies (9 and 34 GHz), which showed that the positions of the resonances were caused by g anisotropy rather than hyperfine coupling. All of the spectra show more than one set of overlapping resonances, indicating the presence of either more than one radical or the same radical in different chemical environments. DFT calculations further substantiated the existence of a single radical per triad. Our model systems, detailed below, revealed that the $(TTFTB)_3$ triad could accommodate a single hole, evenly delocalized across the three TTF cores. Examination of the spin density further suggested that the observed EPR splitting was unlikely to arise from hyperfine coupling. On the basis of this evidence, each organic SBU is best formulated as $(TTFTB)_3^{\bullet 11-}$.

From elemental analysis, we assign the remaining positive charge to a hydronium ion, H_3O^+. An analysis of the electron density and electrostatic potential of hydronium-free **MIT-25**, shown in Figure 2, revealed regions of high potential only in the small pores, suggesting that they likely accommodate the H_3O^+ ions. Indeed, although the small pores are narrow, they are sufficiently large to accommodate H_3O^+ and water. Thus, the balanced overall formula for **MIT-25** is best represented as $Mg_2H_6(H_3O)(TTFTB)_3$, where the $(TTFTB)_3$ triad carries a charge of 11− and the hydronium is found in the small pores.

We conjecture that the radical TTF-based organic SBU is critical in forming the **ssp** net with Mg^{2+}, but is it unique in doing so? To investigate whether other four-connected ligands might give rise to the same net when combined with Mg^{2+} ions, we substituted the TTF core with pyrene, another well-known electron-rich aromatic moiety with a propensity to create interacting aromatic π systems, and investigated the reactivity of 1,3,6,8-tetrakis(*p*-benzoic acid)pyrene (H_4TBAPy)[13] with various Mg^{2+} precursors. Despite systematically changing reaction conditions including temperature, solvent system, and reagent concentration, we were not able to isolate the **ssp** net with H_4TBAPy. Instead, this ligand exclusively formed $[Mg_3(H_3O)_2(TBAPy)_2(\mu_2\text{-}OH_2)_2(H_2O)_2]\cdot 6.5(DMF)\cdot(H_2O)\cdot 0.5(dioxane)$ (**MIT-26**). Crystallizing in space group $P\bar{1}$, **MIT-26** is a two-dimensional MOF wherein neighboring pyrene moieties exhibit short contacts of 3.59 Å but fail to reproduce the triad organic SBUs that are critical for the formation of the **ssp** net (Figure S9). Thus, despite having similar molecular dimensions and geometry, H_4TTFTB and H_4TBAPy form vastly different topologies, highlighting the unique role of the TTF cores and organic SBUs in defining the overall MOF structure.

Insight into the particular role of TTF, especially as contrasted with pyrene, comes from in-depth computational analysis of the electronic structures of the two ligands as well as their supramolecular synthons. The calculated electronic structure of H_4TTFTB is similar to that found for TTF itself, with the electrostatic potential map revealing an electron-rich core centered on the sulfur atoms (Figure S10a). H_4TBAPy exhibits a comparable electronic structure, with electron density localized on the pyrene core (Figure S10c). Stacking of two neutral H_4TTFTB or H_4TBAPy is energetically favored, with formation energies of −1.62 and −1.84 kcal/dimer, respectively (Table 1).

Table 1. Formation Energies for Neutral and Oxidized Dimeric or Trimeric H_4TTFTB and H_4TBAPy Species As Calculated by DFT

species	formation energy (kcal/mol)
$(H_4TTFTB)_2$	−1.62
$(H_4TTFTB)_2^{\bullet+}$	−5.52
$(H_4TTFTB)_3^{\bullet+}$	−13.73
$(H_4TBAPy)_2$	−1.84
$(H_4TBAPy)_2^{\bullet+}$	−4.53

Calculations suggest that both dimers are further stabilized by the presence of a fully delocalized hole, with the formation energies for the oxidized dimers reaching −5.52 and −4.53 kcal/dimer, respectively (Figure 3a,c). Although oxidation by one electron

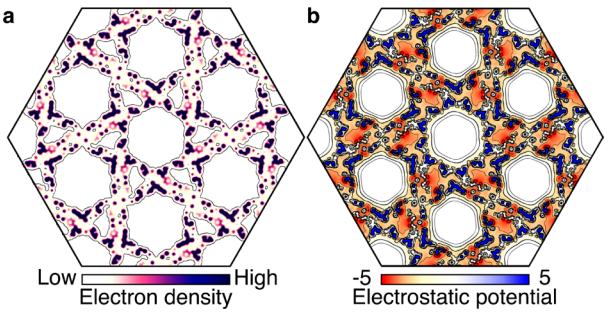

Figure 2. (a) The electron density in both the large and small pores rapidly approaches zero in **MIT-25**. (b) The electrostatic potential plateaus in the large pores to a level defined as zero. In the small pores, the potential is significantly more negative even at the center (red regions). The results shown were computed using a method detailed previously.[12]

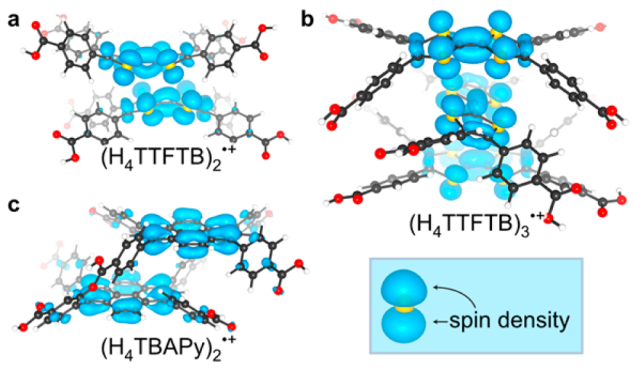

Figure 3. The calculated spin densities ($\rho\uparrow - \rho\downarrow$) of (a) $(H_4TTFTB)_2^{\bullet+}$ and (b) $(H_4TTFTB)_3^{\bullet+}$ showing full hole delocalization across the TTF core. (c) The one-electron-oxidized $(H_4TBAPy)_2^{\bullet+}$ shows similar spin delocalization across the conjugated pyrene core.

DOI: 10.1021/jacs.6b13176
J. Am. Chem. Soc. 2017, 139, 3619–3622

leads to relative stabilization in both cases, only TTF has a readily accessible oxidation potential (E = 0.34 V vs Ag/AgCl in MeCN),[14] whereas TBAPy remains neutral under similar experimental conditions (E = 1.16 V vs SCE in MeCN).[15] Thus, we would not expect H_4TBAPy to oxidize in air to form the hypothetical dimer presented in Figure 3c.

The addition of a second neutral H_4TTFTB ligand to a $(H_4TTFTB)_2^{\bullet+}$ dimer provides significant further stabilization to the $(H_4TTFTB)_3^{\bullet+}$ trimer (13.73 kcal/trimer), with the hole now fully delocalized over all three TTF cores (Figure 3b), a stabilization frequently observed in sulfur-containing conjugated organics.[16] Delocalization of the hole over all three TTF cores in the $(TTFTB)_3^{\bullet11-}$ SBU in **MIT-25** is supported experimentally by X-ray crystallographic analysis, from examination of the C−S and central C═C bond lengths, which vary by only 0.0015 and 0.007 Å, respectively (Table S2). This indicates that all three TTF units in a single triad carry equivalent (partial) oxidation states.[17]

Although the formation of π-interacting motifs provides overall stabilization, as seen with **MIT-26** and numerous other examples,[2] these studies emphasize the importance of accessing oxidized species as well as delocalizing the holes to stabilize organic SBUs. These principles are illustrated in **MIT-25**, whose unique mesoporous structure and new topology arise only because of the organic SBU. The formation of π-stabilized organic SBUs by the deliberate introduction of holes may serve as a general strategy to obtain materials with new topologies.

■ ASSOCIATED CONTENT

Supporting Information

The Supporting Information is available free of charge on the ACS Publications website at DOI: 10.1021/jacs.6b13176.

Procedures and additional data (PDF)
Crystallographic data for **MIT-25** (CIF)
Crystallographic data for **MIT-26** (CIF)
Animation showing the structure of **MIT-25** (GIF)

■ AUTHOR INFORMATION

Corresponding Author

*mdinca@mit.edu

ORCID

Christopher H. Hendon: 0000-0002-7132-768X
Alistair J. Fielding: 0000-0002-4437-9791
Aron Walsh: 0000-0001-5460-7033
Mircea Dincă: 0000-0002-1262-1264

Notes

The authors declare no competing financial interest.

■ ACKNOWLEDGMENTS

All experimental work was supported by the U.S. Department of Energy, Office of Science, Office of Basic Energy Sciences (DE-SC0006937). M.D. gratefully acknowledges early career support from the Sloan Foundation, the Research Corporation for Science Advancement (Cottrell Scholar), and the Dreyfus Foundation. S.S.P. was partially supported by a National Science Foundation Graduate Research Fellowship (1122374). A.J.F. was supported by Bruker. All of the EPR experiments were carried out at the EPSRC National EPR Facility and Service, University of Manchester, U.K.. A.W. was supported by the ERC (277757). S.S.P. thanks M. Korzyński for providing H_4TBAPy. We thank Dr. P. Müller and Dr. J. Becker for assistance with crystallography and Prof. O. Yaghi for valuable discussions. Computational work was enabled by access to XSEDE, which is supported by NSF (ACI-1053575).

■ REFERENCES

(1) (a) Yaghi, O. M.; O'Keeffe, M.; Ockwig, N. W.; Chae, H. K.; Eddaoudi, M.; Kim, J. *Nature* **2003**, *423*, 705. (b) Nouar, F.; Eubank, J. F.; Bousquet, T.; Wojtas, L.; Zaworotko, M. J.; Eddaoudi, M. *J. Am. Chem. Soc.* **2008**, *130*, 1833. (c) Cairns, A. J.; Perman, J. A.; Wojtas, L.; Kravtsov, V. C.; Alkordi, M. H.; Eddaoudi, M.; Zaworotko, M. J. *J. Am. Chem. Soc.* **2008**, *130*, 1560. (d) Tranchemontagne, D. J.; Mendoza-Cortés, J. L.; O'Keeffe, M.; Yaghi, O. M. *Chem. Soc. Rev.* **2009**, *38*, 1257. (e) Yaghi, O. M.; Li, Q. *MRS Bull.* **2009**, *34*, 682. (f) Perry, J. J., IV; Perman, J. A.; Zaworotko, M. J. *Chem. Soc. Rev.* **2009**, *38*, 1400. (g) Mellot-Draznieks, C.; Cheetham, A. K. *Nat. Chem.* **2017**, *9*, 6.

(2) (a) Amabilino, D. B.; Stoddart, J. F. *Chem. Rev.* **1995**, *95*, 2725. (b) Claessens, C. G.; Stoddart, J. F. *J. Phys. Org. Chem.* **1997**, *10*, 254. (c) Chen, B.; Eddaoudi, M.; Hyde, S. T.; O'Keeffe, M.; Yaghi, O. M. *Science* **2001**, *291*, 1021. (d) Dincă, M.; Dailly, A.; Tsay, C.; Long, J. R. *Inorg. Chem.* **2008**, *47*, 11. (e) Reger, D. L.; Horger, J.; Smith, M. D.; Long, G. J. *Chem. Commun.* **2009**, *41*, 6219. (f) Nakano, T. *Polym. J.* **2010**, *42*, 103. (g) Chen, T.-H.; Popov, I.; Miljanić, O. Š. *Chem. - Eur. J.* **2017**, *23*, 286.

(3) (a) Govers, H. A. J.; de Kruif, C. G. *Acta Crystallogr., Sect. A: Cryst. Phys., Diffr., Theor. Gen. Crystallogr.* **1980**, *36*, 428. (b) Hunter, C. A.; Sanders, J. K. M. *J. Am. Chem. Soc.* **1990**, *112*, 5525. (c) Martinez, C. R.; Iverson, B. L. *Chem. Sci.* **2012**, *3*, 2191.

(4) (a) Kollman, P. A.; Allen, L. C. *J. Chem. Phys.* **1969**, *51*, 3286. (b) Smith, J. D.; Cappa, C. D.; Wilson, K. R.; Messer, B. M.; Cohen, R. C.; Saykally, R. J. *Science* **2004**, *306*, 851.

(5) (a) Rodgers, M. T.; Armentrout, P. B. *Mass Spectrom. Rev.* **2000**, *19*, 215. (b) Armentrout, P. B.; Halle, L. F.; Beauchamp, J. L. *J. Am. Chem. Soc.* **1981**, *103*, 6501.

(6) (a) Narayan, T. C.; Miyakai, T.; Seki, S.; Dincă, M. *J. Am. Chem. Soc.* **2012**, *134*, 12932−12935. (b) Park, S. S.; Hontz, E. R.; Sun, L.; Hendon, C. H.; Walsh, A.; Van Voorhis, T.; Dincă, M. *J. Am. Chem. Soc.* **2015**, *137*, 1774.

(7) Barrett, E. P.; Joyner, L. G.; Halenda, P. P. *J. Am. Chem. Soc.* **1951**, *73*, 373.

(8) Kruk, M.; Jaroniec, M.; Sayari, A. *Langmuir* **1997**, *13*, 6267.

(9) Brunauer, S.; Emmett, P. H.; Teller, E. *J. Am. Chem. Soc.* **1938**, *60*, 309.

(10) Deng, H.; Grunder, S.; Cordova, K. E.; Valente, C.; Furukawa, H.; Hmadeh, M.; Gándara, F.; Whalley, A. C.; Liu, Z.; Asahina, S.; Kazumori, H.; O'Keeffe, M.; Terasaki, O.; Stoddart, J. F.; Yaghi, O. M. *Science* **2012**, *336*, 1018.

(11) Chatgilialoglu, C.; Asmus, K.-D. *Sulfur-Centered Reactive Intermediates in Chemistry and Biology*; Springer: New York, 2013.

(12) (a) Walsh, A.; Butler, K. T.; Hendon, C. H. *MRS Bull.* **2016**, *41*, 870. (b) Butler, K. T.; Hendon, C. H.; Walsh, A. *J. Am. Chem. Soc.* **2014**, *136*, 2703. The codes are available from https://github.com/WMD-group/MacroDensity (accessed Feb 28, 2017).

(13) Stylianou, K. C.; Heck, R.; Chong, S. Y.; Bacsa, J.; Jones, J. T. A.; Khimyak, Y. Z.; Bradshaw, D.; Rosseinsky, M. J. *J. Am. Chem. Soc.* **2010**, *132*, 4119.

(14) Bendikov, M.; Wudl, F.; Perepichka, D. F. *Chem. Rev.* **2004**, *104*, 4891.

(15) Murov, S. L.; Carmichael, I.; Hug, G. L. *Handbook of Photochemistry*; Marcel Dekker: New York, 1993.

(16) Hendon, C. H.; Carbery, D. R.; Walsh, A. *Chem. Sci.* **2014**, *5*, 1390.

(17) (a) Cooper, W. F.; Kenny, N. C.; Edmonds, J. W.; Nagel, A.; Wudl, F.; Coppens, P. *J. Chem. Soc. D* **1971**, *16*, 889. (b) Kistenmacher, T. J.; Phillips, T. E.; Cowan, D. O. *Acta Crystallogr., Sect. B: Struct. Crystallogr. Cryst. Chem.* **1974**, *30*, 763. (c) Clemente, D. A.; Marzotto, A. *J. Mater. Chem.* **1996**, *6*, 941.

DOI: 10.1021/jacs.6b13176
J. Am. Chem. Soc. 2017, 139, 3619−3622